

Table 1 (continued).

Mouse	Pick	Tree*	Cells picked	Total sequences†	Total unique sequences‡	Mutations per unique sequence	Trunk§ mutations per unique sequence	Branch mutations per unique sequence	
								Shared	Unique¶
7983	17a3	A	5	3	1	4.0	<b>4.0</b>	0.0	0.0
		B		3	1	4.0	<b>4.0</b>	0.0	0.0
	17a4	C	10	3	2	4.5	4.0	0.0	0.5
		D		4	2	1.5	1.0	0.0	0.5
		E		1	1	1.0	<b>1.0</b>	0.0	0.0
	17a5	F	50	1	1	1.0	<b>1.0</b>	0.0	0.0
		G		8	6#	3.0	0.0	0.8	2.2
	17b1	H	10	2	1	6.0	<b>6.0</b>	0.0	0.0
		I		5	1	5.0	<b>5.0</b>	0.0	0.0
Total			853	305	125				
Weighted average						4.3	3.2	0.4	0.7

\*Genealogical tree to which sequences in a pick are assigned. Equivalent letters in an individual mouse are part of the same tree. †All sequences derived from a pick. ‡Total number of different sequences in a pick. §Mutations shared by all of the clones on a tree and preceding branch mutations. ||Mutations that are seen in multiple sequences of a pick. ¶Mutations that occur in only one unique sequence of a pick. #Trees containing one or more germline sequences. All mutations present in such trees are counted as branch mutations.

ulate through unique pathways, B cells may mutate elsewhere (25) and thereby escape the mechanisms that normally censor autoreactive B cells in the GC environment.

References and Notes

- M. J. Shlomchik, J. Craft, M. J. Mamula, *Nature Rev. Immunol.* **1**, 147 (2001).
- M. J. Shlomchik, D. Zharhary, T. Saunders, S. Camper, M. Weigert, *Int. Immunol.* **5**, 1329 (1993).
- L. G. Hannum, D. Ni, A. M. Haberman, M. G. Weigert, M. J. Shlomchik, *J. Exp. Med.* **184**, 1269 (1996).
- H. Wang, M. J. Shlomchik, *J. Exp. Med.* **190**, 639 (1999).

- M. J. Shlomchik, A. Marshak-Rothstein, C. B. Wolfowicz, T. L. Rothstein, M. G. Weigert, *Nature* **328**, 805 (1987).
- M. J. Shlomchik *et al.*, *J. Exp. Med.* **171**, 265 (1990).
- Materials and methods are available as supporting material on *Science* Online.
- J. William, C. Euler, S. Christensen, M. J. Shlomchik, unpublished observations.
- J. William, C. Euler, M. J. Shlomchik, in preparation.
- J. William, C. Euler, S. Christensen, M. J. Shlomchik, in preparation.
- C. Garcia De Vinuesa *et al.*, *Eur. J. Immunol.* **29**, 3712 (1999).
- Cells were captured with a glass micropipette attached to an Eppendorf Transferman micromanipula-

tor. Vκ8/J4 rearranged sequences were amplified by nested PCR using Pfu Turbo (Stratagene). Amplified DNA was cloned and further amplified by picking transformed colonies directly into a PCR amplification reaction using M13 external primers. The PCR product was then purified and sequenced with a T3 primer. See supporting online material for details.

- R. Thiebe *et al.*, *Eur. J. Immunol.* **29**, 2072 (1999).
- S. Kleinstein, Y. Louzoun, unpublished data.
- S. Weller *et al.*, *Proc. Natl. Acad. Sci. U.S.A.* **98**, 1166 (2001).
- M. Matsumoto *et al.*, *Nature* **382**, 462 (1996).
- K. G. Smith, G. J. Nossal, D. M. Tarlinton, *Proc. Natl. Acad. Sci. U.S.A.* **92**, 11628 (1995).
- Y. Takahashi, H. Ohta, T. Takemori, *Immunity* **14**, 181 (2001).
- E. Kallberg, S. Jainandunsing, D. Gray, T. Leanderson, *Science* **271**, 1285 (1996).
- D. Watanabe, T. Suda, S. Nagata, *Int. Immunol.* **7**, 1949 (1995).
- E. A. Leadbetter *et al.*, *Nature* **416**, 603 (2002).
- K. M. Shokat, C. C. Goodnow, *Nature* **375**, 334 (1995).
- S. Han *et al.*, *J. Immunol.* **155**, 556 (1995).
- B. Pulendran, K. G. C. Smith, G. J. V. Nossal, *J. Immunol.* **155**, 1141 (1995).
- A. E. Schroder, A. Greiner, C. Seyfert, C. Berek, *Proc. Natl. Acad. Sci. U.S.A.* **93**, 221 (1996).
- We thank A. Haberman, J. Craft, M. Nussenzweig, and M. Weigert for critical reading of the manuscript; A. Rothstein for useful discussions; S. Kleinstein and Y. Louzoun for collaboration on mutation rate calculations and sharing their unpublished results; and W. DeLage for expert animal care. Supported by grant P01-A36529 from NIH.

Supporting Online Material

[www.sciencemag.org/cgi/content/full/297/5589/2066/DC1](http://www.sciencemag.org/cgi/content/full/297/5589/2066/DC1)  
 Materials and Methods  
 Figs. S1 to S3  
 Tables S1 and S2  
 Reference S1

14 May 2002; accepted 10 July 2002

# Coordinated Reactivation of Distributed Memory Traces in Primate Neocortex

K. L. Hoffman and B. L. McNaughton

Conversion of new memories into a lasting form may involve the gradual refinement and linking together of neural representations stored widely throughout neocortex. This consolidation process may require coordinated reactivation of distributed components of memory traces while the cortex is “offline,” i.e., not engaged in processing external stimuli. Simultaneous neural ensemble recordings from four sites in the macaque neocortex revealed such coordinated reactivation. In motor, somatosensory, and parietal cortex (but not prefrontal cortex), the behaviorally induced correlation structure and temporal patterning of neural ensembles within and between regions were preserved, confirming a major tenet of the trace-reactivation theory of memory consolidation.

Our ability to recall detailed memories, even from the distant past, suggests that we have a robust, high-capacity neural system for storing memories. Yet, in the minutes to days

after an event, memory for that event is susceptible to disruption. This period of lability may be a consequence of the way memory traces are stored throughout the cortex.

Marr (1) was perhaps the first to suggest how a sparsely connected hierarchical network such as the cortex may be capable of high-capacity, detailed representation, with the caveat that the final memory trace is not

made entirely “on-the-fly” (2–5). Instead, after an event occurs, a top-down cascade of neural activity may ensue. Event-related activity in cells from higher level regions of cortex (e.g., hippocampus and related associational structures) may elicit activity in cells from lower level regions that were also active during the event. Through repeated coactivation, these lower level ensembles may create the connections necessary to encode the memory trace efficiently and to sustain it, or some approximation of it, independently of top-down input. This “trace-reactivation” theory is one of several theories that explain the protracted period of time required for memory consolidation and why cortical association areas, such as the hippocampus, are necessary during such consolidation periods. Two critical predictions follow from this theory: (i) Patterns of neural ensemble activity expressed during an experience should be spontaneously reactivated during subsequent periods of behavioral inactivity; and (ii) the distributed components of the reactivated memory trace should appear concurrently within the relevant cortical sites.

Consistent with the former prediction, neural ensembles in the rat hippocampus and

Division of Neural Systems, Memory, and Aging, University of Arizona, Tucson, AZ 85724, USA.

\*To whom correspondence should be addressed. E-mail: bruce@nsma.arizona.edu

## REPORTS

neocortex show memory trace reactivation during “offline periods” of quiet wakefulness, slow-wave sleep, and in some cases REM (rapid eye movement) sleep (6–9). Reactivation of recent memory traces is also observed during sleep in motor areas of the zebra finch brain (10). Finally, neuroimaging in humans reveals that brain areas with increased signal during a task have continued or reappearing activity after the task is completed (11). Unfortunately, the spatial and temporal resolution of imaging methods such as positron emission tomography and magnetic resonance does not permit the identification of which neurons within a brain region are active as part of a memory trace.

To date, only one study has addressed the second prediction, revealing concurrent reactivation of neural ensembles between the hippocampus and parietal cortex of rats (12). Whether separate neocortical areas less directly connected to the hippocampus reactivate memory traces concurrently is not yet known. Furthermore, achieving concurrent reactivation among neocortical areas is even more problematic in the primate brain, owing to the increase in the number of neurons and neocortical processing modules and the consequent reduction in net overall connectivity.

To address the foregoing question, we implanted an array of 144 independently advanceable microelectrodes into each of four regions of the primate neocortex: posterior parietal cortex (PP), motor cortex (M), somatosensory cortex (SS), and dorsal prefrontal cortex (PFC) (13) (Fig. 1). Each array consisted of a 12 by 12 lattice of electrodes with a 650- $\mu$ m spacing. Multiple individual neurons were recorded simultaneously during

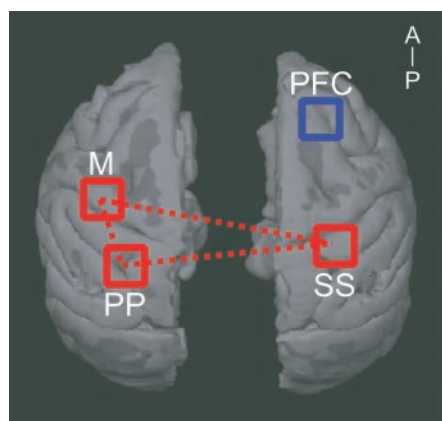


**Fig. 1.** Dorsal view of electrode recording sites registered to a preoperative magnetic resonance image. Brain regions sampled include dorsal prefrontal cortex (PFC), somatosensory cortex (SS), posterior parietal cortex (PP), and motor cortex (M). Each square represents the area covered by a chronically implanted 12 by 12 array of electrodes. Red squares indicate the areas that showed memory trace reactivation; red dotted lines indicate regions that reactivated together. AP: anterior, posterior.

30 min of rest (Rest 1), a sequential reaching behavior (Task), and a final 30 min of rest (Rest 2). Studies in rodents show that reactivation measures decline substantially over about 30 min after the performance of a task; therefore, analysis of rest data was restricted to the 10 min of Rest 1 and Rest 2 immediately flanking the task.

A total of 800 cells (20, 253, 243, and 284 cells from PP, M, SS, and PFC, respectively) were isolated over nine recording sessions, producing a total of 21,288 cell pairs eligible for correlation analyses. Cells in all four areas exhibited firing modulation related to task events (Fig. 2), and there was no significant difference in the mean firing rates of cells by brain region or by behavioral epoch, although firing rates tended to be slightly higher during the task.

If reactivation occurs, cells that were active together during the task should tend to be coactive afterward, and cells active at different times during the task should not be coactive afterward. Such reemergence of neural coactivity patterns can be quantified by computing how much of the variance in the distribution of cell-pair correlations during Rest 2 can be explained statistically by the pattern of correlations induced during Task after factoring out the distribution of correlations already present in the baseline period [i.e., Rest 1 (13)]. Cell-pair correlations were obtained by calculating Pearson’s correlation coefficient from the binned spike trains of all eligible pairs of cells for each epoch (Fig. 3B). The explained variance (EV) was then calculated from the partial regression of Task and

Rest 2 cell-pair correlations controlling for those of Rest 1 (6, 12, 13). When the correlations from all nine sessions were pooled by epoch, the overall EV was significantly greater than the epoch-swapped control levels [ $P < 0.05$  (13)]. Substantial EV was apparent across most sessions but not across all brain regions (Fig. 3C).

Correlations based on all combinations of cell pairs from the same array (i.e., within-area correlations) produced a significant difference in EV for PP ( $P = 0.023$ ), M ( $P = 0.0002$ ), and SS ( $P = 0.0006$ ). Significant EV above control EV was also evident across brain regions for correlations of PP-M pairs ( $P = 0.017$ ), PP-SS pairs ( $P = 0.029$ ), and M-SS pairs ( $P = 0.001$ ). In contrast, the activity of PFC cells paired within or across areas did not lead to significant EV above control levels (PFC,  $P = 0.468$ ; PP-PFC,  $P = 0.1841$ ; M-PFC,  $P = 0.095$ ; SS-PFC,  $P = 0.8810$ ).

The extent to which sequences of activity were preserved during reactivation was also assessed. For each epoch, cross-correlograms (CCGs) were calculated by grouping spikes into 10-ms bins and calculating the correlation between all cell pairs over  $\pm 1$ -s time lags (13). When one cell tends to fire before another cell as a consequence of the task, temporal bias appears as an offset, or asymmetry, in the CCG peak. If the temporal biases of Task CCGs are more similar to those of Rest 2 CCGs than those of Rest 1 CCGs, this indicates the presence of some degree of sequence reactivation (Fig. 4A). By this criterion, significant reactivation of se-

**Fig. 2.** Task-related neural activity. (A) Cell-by-time firing rate matrix from somatosensory cortex within the first 5 min of one task. The task was repeated approximately every 40 s, matching the response periodicity of several cells. Periodic responses continued for the duration of the task (not shown). Firing rates are truncated at 10 Hz for illustrative purposes. (B) Peri-event time histograms of neural firing related to 52 juice reward events from the alley maze task. Juice delivery was preceded by a successful touch of the touchscreen cue. After a correct touch, the monkey retracted his arm and consumed the juice before resuming lever pulling. Task-related activity was present in all four brain regions, and a variety of response types was seen in each region. About 20% of the cells examined had event-related activity of similar magnitude to those shown here, indicating that neurons were in some way responsive to elements of the task.

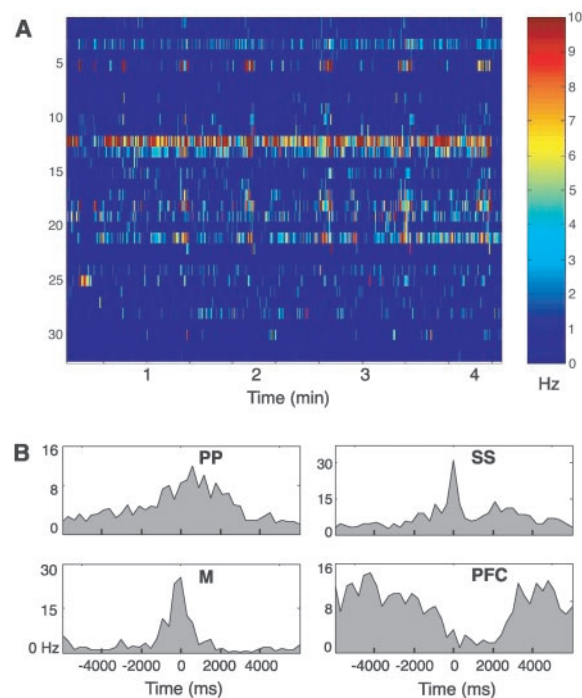
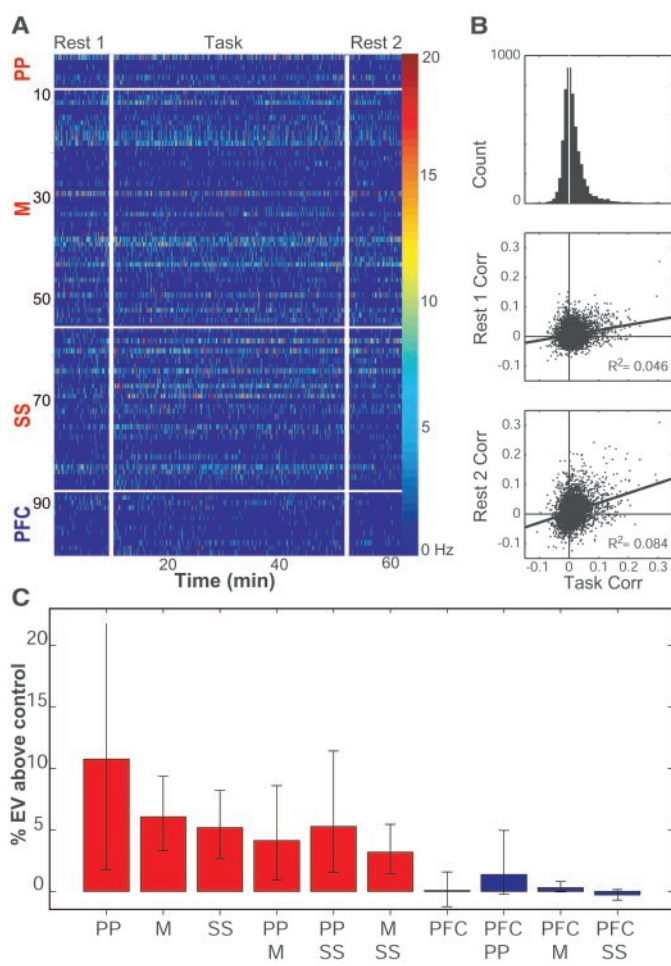


**Fig. 3.** Quantification of memory trace reactivation based on cell-pair firing rate correlation distributions. **(A)** Cell-by-time firing rate matrix from one recording session of 99 simultaneously recorded cells. Each row represents the binned firing rate of one cell, positioned according to brain region. Each column represents the firing rate of each cell at a given bin of time. For illustrative purposes, firing rates were truncated at 20 Hz. **(B)** For each epoch, rate-independent cell-pair correlations were made for all eligible pairs of cells ( $n = 4838$ ). (Top) Histogram of cell-pair correlations during the Task epoch. (Middle) Cell-pair correlations of Task versus Rest 1. (Bottom) Cell-pair correlations of Task versus Rest 2. The cell-pair correlations during Task are more similar to those of Rest 2 than to those of Rest 1 ( $P < 0.001$ ). **(C)** Explained variances (EV) of cell-pair correlations from pairs within and across brain regions after subtraction of the control values. Error bars represent 95% confidence limits. All red bars, and no blue bars, are significant ( $P < 0.05$ ).



quences of neural ensemble activity was observed within M and SS but not within PFC (Fig. 4B). Reactivation of sequences was also seen between PP and M, but not between M and SS nor between any combination that included PFC cells.

In agreement with a widely held hypothesis concerning the mechanisms of memory consolidation, the results of this study demonstrate that memory trace reactivation occurs in a coherent, distributed manner across much of the neocortex. The observed explained variance and temporal bias effects were small, as would be expected if the reactivation process was neither precise nor exclusive to the immediately preceding Task events. The preservation of correlation structure and temporal bias, however, does indicate that, during the rest epochs, the ensemble activity fluctuated among many recently experienced activity states, at least partly in the original temporal sequence. Thus, the observed effects reflect a reactivation of previous events and not merely a persistence of a fixed activity state. Previous studies of the rat hippocampus showed that correlation patterns during two sequentially experienced mazes were both reactivated in subsequent rest, and that a small degree of reactivation could be observed at least 24 hours after the task was performed (6). These and the present results indicate that the observed effect is not simply an uninterrupted persistence of a previously expressed activity state, but rather reflects the reemergence of recent patterns. The current methods, however, cannot distinguish whether the low values of EV and bias preservation result from imperfect recall of recent patterns or from an interleaving of recent memories with other activity states, possibly including other memory traces.

Cells recorded in dorsal PFC showed no signs of memory trace reactivation. This result seems to contrast with the evidence from neuroimaging literature that right dorsal PFC is active during episodic memory retrieval in humans; however, this region may become active in memory tasks as part of a cognitive set associated with intentional retrieval, rather than retrieval per se (14), and is active for a variety of other tasks requiring working memory and/or monitoring functions (15). The PFC may facilitate intentional memory retrieval only through its role in short-term mnemonic, executive, or monitoring functions, which may not be stored as components of an episodic memory. Alternatively, the dorsal PFC may be capable of offline reprocessing, given tasks that generate the necessary kinds of network activity for creating memory traces. Although in the present tasks the firing rates and task-related modulations in PFC were similar to those seen in the other areas, other critical characteristics of ensemble firing dynamics or neuromodulatory influences may have been absent. Fur-

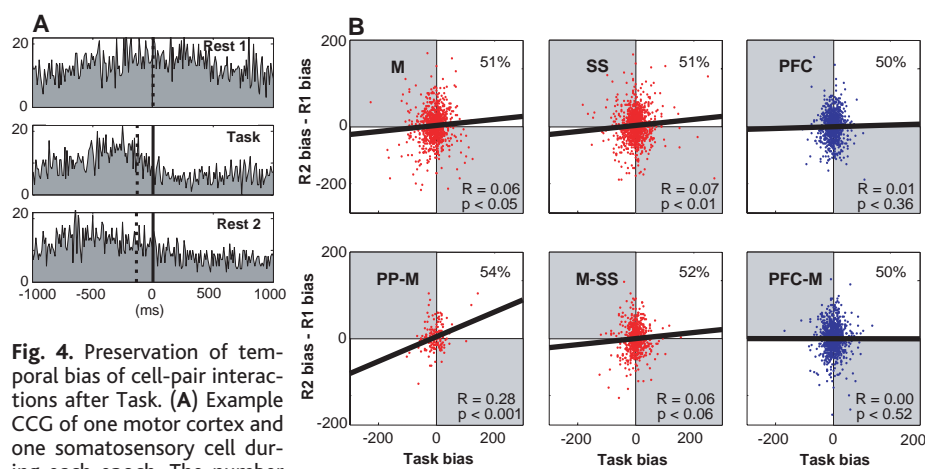


**Fig. 4.** Preservation of temporal bias of cell-pair interactions after Task. **(A)** Example CCG of one motor cortex and one somatosensory cell during each epoch. The number of coincidences within each 10-ms bin is plotted. The bias (dotted black line) during Rest 2 (bottom) is similar to the bias evoked by the task (middle), which was different from rest beforehand (top). **(B)** Distributions of temporal bias during Task and Rest epochs. The bias during task is plotted against the difference in biases of Rest 2 and Rest 1. Within-region CCG biases are plotted in the first row, and between-region biases are plotted in the second row. The proportion of CCGs with preserved temporal bias (those falling in the white quadrants) is listed in the upper right quadrant. For significant correlations, the majority of points fall in the white quadrants, indicating that the correlation is not driven strictly by the magnitude of outliers.

## REPORTS

ther studies will be required to clarify the role, if any, of PFC in spontaneous memory trace reactivation.

At present, the mechanisms leading to the observed widespread memory trace reactivation remain unknown, and the necessity of coherent memory trace reactivation for memory consolidation remains to be demonstrated. Nevertheless, the observation that memory trace reactivation is temporally ordered and concurrent across large areas of the primate neocortex is a critical prerequisite for this process to function as a mechanism for memory consolidation.

### References and Notes

1. D. Marr, *Philos. Trans. R. Soc. London Ser. B* **262**, 23 (1971).
2. L. R. Squire, N. J. Cohen, L. Nadel, in *Memory Consol-*

- idation*, G. Weingartner, E. Parker, Eds. (Erlbaum, Hillsdale, NJ, 1984), pp. 185–210.
3. G. Buzsaki, *Neuroscience* **31**, 551 (1989).
4. A. Treves, E. T. Rolls, *Hippocampus* **4**, 374 (1994).
5. J. L. McClelland, B. L. McNaughton, R. C. O'Reilly, *Psychol. Rev.* **102**, 419 (1995).
6. H. S. Kudrimoti, C. A. Barnes, B. L. McNaughton, *J. Neurosci.* **19**, 4090 (1999).
7. K. Louie, M. A. Wilson, *Neuron* **29**, 145 (2001).
8. M. A. Wilson, B. L. McNaughton, *Science* **265**, 676 (1994).
9. Z. Nadasdy, H. Hirase, A. Czurko, J. Csicsvari, G. Buzsaki, *J. Neurosci.* **19**, 9497 (1999).
10. A. S. Dave, D. Margoliash, *Science* **290**, 812 (2000).
11. P. Maquet *et al.*, *Nature Neurosci.* **3**, 831 (2000).
12. Y. L. Qin, B. L. McNaughton, W. E. Skaggs, C. A. Barnes, *Philos. Trans. R. Soc. London Ser. B* **352**, 1525 (1997).
13. Materials and methods are available as supporting material on *Science* Online.
14. M. LePage, O. Ghaffar, L. Nyberg, E. Tulving, *Proc. Natl. Acad. Sci. U.S.A.* **97**, 506 (2000).
15. A. K. MacLeod, R. L. Buckner, F. M. Miezin, S. E. Petersen, M. E. Raichle, *Neuroimage* **7**, 41 (1998).

16. We thank A. Gmitro and the Flynn Biological MRI/MRS Program for assistance with magnetic resonance (MR) and computerized tomography (CT) image acquisition; T. M. Ellmore for MR and CT image processing; F. Battaglia, J. de Dios, K. Hardesty, G. Lewandowski, P. Lipa, M. Newton, and K. Spitzer for technical assistance; K. Stengel and Neuralynx Inc. for developments in recording technology; and C. Barnes, K. Gothard, and L. Nadel for helpful comments on the manuscript. K.L.H. was supported by an NSF Predoctoral Fellowship. This work was supported by a grant from Japan Science and Technology Corporation–Core Research for Evolutional Science and Technology and by grant MH01565 from the National Institute of Mental Health and was performed in partial fulfillment of a Ph.D. dissertation.

### Supporting Online Material

[www.sciencemag.org/cgi/content/full/297/5589/2070/DC1](http://www.sciencemag.org/cgi/content/full/297/5589/2070/DC1)

Materials and Methods  
Figs. S1 to S5  
Table S1

2 May 2002; accepted 7 August 2002

# Science *sets the pace*

online manuscript submission

**MANUSCRIPTS** [www.submit2science.org](http://www.submit2science.org)

Science can now receive and review all manuscripts electronically

online letter submission

**LETTERS** [www.letter2science.org](http://www.letter2science.org)

Have your voice be heard immediately



## *speed submission*